Nano-magnetic potassium impregnated ceria as catalyst for the biodiesel production

Ambat Indu, Srivastava Varsha, Haapaniemi Esa, Sillanpää Mika

DOI: 10.1016/j.renene.2019.03.042

Nano-magnetic potassium impregnated ceria as catalyst for the biodiesel production.

Indu Ambat [a]*, Varsha Srivastava [a], Esa Haapaniemi [c], Mika Sillanpää [a, b]

[a] Department of Green Chemistry, School of Engineering Science, Lappeenranta University of Technology, Sammonkatu 12, FI-50130 Mikkeli, Finland

[b] Department of Civil and Environmental Engineering, Florida International University, Miami, FL-33174, USA

[c] Department of Organic Chemistry, University of Jyväskylä, Finland

*Corresponding Author (email: indu.ambat@lut.fi)

Abstract

The main objective of this work comprises the investigation of biodiesel production from rapeseed oil using potassium impregnated Fe_3O_4-CeO_2 nanocatalyst. The various concentration of potassium impregnated Fe_3O_4-CeO_2 was screened for catalytic conversion of rapeseed oil to triglyceride methyl ester. The 25 wt % potassium impregnated Fe_3O_4-CeO_2 nanocatalyst showed best biodiesel production. Nanocatalyst was characterized by FTIR, XRD, SEM, TEM, BET and Hammett indicator for basicity test. The characterization of biodiesel was performed with GC-MS, ^{1}H and ^{13}C NMR. Moreover, the optimum reaction parameters such as catalyst amount (wt %), oil to methanol ratio, reaction time and reaction temperature for transesterification reaction was analyzed and yield was determined by ^{1}H NMR. The maximum yield of 96.13 % was obtained at 4.5 wt % catalyst amount, 1:7 oil to methanol ratio at 65 °C for 120 minutes. The properties of biodiesel such as acid value and kinematic viscosity were observed as 0.308 mg KOH/g and 4.37 mm^2/s respectively. The other fuel parameters such as flash point and density were also determined. The reusability of catalyst was observed and it showed stability up to five cycles without considerable loss of activity. The recovery of excess methanol after transesterification reaction was achieved using distillation process setup.

.

Key words: Biodiesel, rapeseed oil, transesterification, Fe_3O_4-CeO_2 nanocatalyst

1. Introduction

Now a days, the inadequacy of conventional fuels along with global warming and direct environmental pollution due to massive utilization of fossil fuels leads to the consideration of an alternative fuel for fossil fuels [1,2]. Biodiesel is fatty acid methyl esters obtained after transesterification of oils with methanol [3].

Biodiesel is one of the alternative fuel, which possess all the properties such as renewability, accessibility, sustainable nature, and clean fuel that can meet all the challenges caused by fossil fuels [4,5]. Furthermore, domestically available numerous sources such as vegetable oils, algal oils and animal fat / oils are used as feedstock for the biodiesel production [6] . Various techniques involved in conversion of oils to biodiesel which includes pyrolysis, transesterification, supercritical fluid, and dilution [3,7]. Out of these methodologies most commonly and commercially used is transesterification techniques with homogeneous catalyst. Moreover, there are various catalyst involved in biodiesel production such as homogeneous, heterogeneous and enzyme catalyst [3, 7, 8]. However, the environmental concern related to usage of homogenous catalyst such as huge amount of chemical waste water, whereas solid heterogeneous and enzyme catalyst have various challenges such as mass transfer resistant, reusability of catalyst. [7, 9, 10].

In recent times nanocatalyst attained special attention in various process such as water treatment, drug delivery, optoelectronics and biodiesel production [4, 8, 11-13]. Futhermore nanocatlayst plays a major role in biodiesel production due to its various features such as high stability, efficient catalytic activity, easy operational procedure, reusability, and high surface area [8, 10, 13]. The selection of feedstock for biodiesel production is reliant on the region. For example, in Europe and tropical countries major sources for the production of biodiesel are rapeseed oil and palm oil respectively where as in soybean oil serves as one of the major sources of biodiesel in the United States [3, 13].

The focus of this work is to synthesize potassium impregnated nano-magnetic ceria and use this catalyst for the production of biodiesel from rapeseed oil. The magnetic nanoparticles helps in easy separation of catalyst and increases its reusability [14, 15]. Nanomagnetic particles has been explored as a catalyst in various fields such as water treatment, bio catalysis, photocatalysis but rarely used in field of biodiesel production [16- 19]. Furthermore, as far as our knowledge the transesterification using the potassium impregnated nano-magnetic ceria has not been reported in the literature. The selection of rapeseed oil as a feedstock for biodiesel production is because of its easy availability and comparatively low cost oil in Europe. The CeO_2 magnetic nanoparticles were impregnated with various concentration of potassium ions to determine the doping effect of potassium ions on catalytic activity. The cerium oxide was used in combination with various metal oxides for transesterification reaction [37, 38]. Moreover, ceria was used as catalyst for various catalytic reactions [15, 39]. The characterization of synthesized nanocatalyst was done using FTIR, XRD, SEM, TEM, BET. Further, the nanocatalyst has been used for transesterification reaction, where the production conditions such as temperature molar ratio of oil and methanol, catalyst amount and time were optimized. The biodiesel was analyzed by GC-MS, ^{1}H and ^{13}C NMR.

2. Materials and methods

2.1 Materials

Rapeseed oil (FFA % = 0.442, average molecular weight=892.27), Cerium (III) nitrate hexahydrate (Ce $(NO_3)_3.6H_2O$.), Ferrous chloride tetrahydrate ($FeCl_2$. $4H_2O$) Ferric chloride hexahydrate ($FeCl_3.6H_2O$), Ammonia solution, potassium hydroxide (KOH), methanol of analytical grade were purchased from Sigma-aldrich.

2.2 Synthesis and screening of catalyst

The magnetic nanoparticles loaded with 25 wt % of ceria was synthesized by co-precipitation of $FeCl_2.4H_2O$, $FeCl_3.6H_2O$, and Ce $(NO_3)_3.6H_2O$ using 25 % ammonia solution. The resulted solution was centrifuged and washed several times with water. The obtained precipitate was dried at 60 °C for 24 h and calcinated at 400 °C in muffle furnace (Nabérthermb180) for 4 hours. The prepared magnetic nanoparticles loaded with 25 wt % ceria was impregnated with different concentration of KOH solution (15, 25, 50 wt %) and stirred continuously for 8h and later dried at 50 °C for overnight. The dried samples were calcined at 500 °C in muffle furnace for 4 hours. A series of potassium impregnated magnetic cerium dioxide nanocatalysts were screened for fatty acid methyl ester (FAME) production from rapeseed oil.

2.3 Characterization of catalyst

FTIR peaks and XRD patterns of synthesized catalyst were examined with Vertex 70 Bruker and PANalytical – Empyrean X-ray diffractometer respectively. SEM images of catalysts were obtained by spreading sample on colloidal graphite with 5 kV accelerating voltage (SEM, Hitachi SU3500). TEM images of the samples were captured using HT7700 (Hitachi).For attaining TEM images the nanocatalyst was dispersed in ethanol and sonicated for 25 minutes and a drop of suspension was added to carbon coated copper grid. Surface area of synthesized catalysts were determined using BET surface area analyzer (BET, Micromeritics Tristar II plus). Prior to perform BET analysis the catalyst samples were degassed at 35 °C for overnight to remove the moisture from the samples.

The basicity of catalyst was determined with help of Hammett indicator. For basicity test analysis , 350 mg of each catalyst was mixed with 1mL of Hammett indicators such as bromothymol blue (H_7.2), phenolphthalein (H_9.8), 2, 4 - dinitroaniline (H_15) and 4-nitroaniline were diluted separately in 10mL of methanol. Later all the samples were kept for 3hours to settle. The catalyst colour was observed after equilibration time. The catalyst experience colour change indicates that the basicity of catalyst was greater than the weakest indicator whereas no colour change shows that the basic strength of catalyst lower than the strongest indicator. [20, 21].

2.4 Biodiesel production using potassium impregnated Fe_3O_4-CeO_2

Rapeseed oil was used as feedstock for biodiesel production. The fatty acid methyl ester production from rapeseed oil using different catalyst was done by mixing methanol to oil in 7:1 molar ratio and with 3wt % of each catalyst. The best catalyst for biodiesel production was selected by conducting all the reactions in a 250mL three neck round bottom flask with mechanical stirrer and reflux condenser at 60 °C for 120 minutes. The separation of fatty acid methyl ester as well as recovery of excess methanol and catalyst by centrifugation of samples after each reaction. The biodiesel was analyzed by GC-MS (Agilent-GC6890N, MS 5975) with agilent DB-wax FAME analysis GC column dimensions 30 m, 0.25 mm, 0.25 µm. The inlet temperature was 250 °C and oven temperature was programmed at 50 °C for 1 minute and it raises at the rate of 25 °C/minute to 200 °C and 3 °C /minute to 230 °C and then it was held for 23 minute. Besides, esters of rapeseed oil after transesterification reaction was analyzed by ^1H and ^{13}C NMR (Bruker). For NMR analysis, fatty acid methyl esters were analyzed by ^1H NMR and ^{13}C NMR at 400 MHz with $CDCl_3$ as solvent .The percentage of conversion of rapeseed oil to fatty acid methyl esters (C %) and percentage of biodiesel yield are determined by the equation (1) and equation (2) respectively [9, 13, 20, 22].

$$C(\%) = \frac{2 \times Intergration\ value\ of\ protons\ of\ methyl\ ester}{3 \times Intergraton\ value\ of\ methyl\ protons} \times 100 \quad (Eq.1)$$

$$Biodiesel\ yield\ (\%) = \frac{mass\ of\ biodiesel}{mass\ of\ oil} \times 100 \quad (Eq.2)$$

Moreover, the transesterification reaction was sustained with the best catalyst attained after screening process. However, the biodiesel production was also effected by reaction parameters such as amount of catalyst oil to methanol ratio, temperature and reaction time.

3. Results and discussion

3.1. Screening and selection of nanocatalyst for biodiesel production from rapeseed oil

The catalytic performance of different catalyst such as 15, 25, 50 wt % potassium impregnated Fe_3O_4-CeO_2 were analyzed for the selection of nanocatalyst for the biodiesel production from rapeseed oil at 60 °C by using 3 wt % catalyst and 1:5 oil to methanol molar ratio within120minutes of reaction time. The catalytic activity of each catalyst was indicated in Fig1. This is due to the optimum loading of potassium ions to Fe_3O_4-CeO_2, which offers sufficient active sites for the fatty acids to bind with the catalyst as well as the basic nature of the catalyst. Moreover the increased amount of KOH above the optimum value, basicity probably decrease the surface basic sites which led to a fall in the catalytic activity of the catalyst with subsequent reduction in yield [21, 23, 24]. The 25 wt % potassium impregnated Fe_3O_4-CeO_2 [named as Fe_3O_4-CeO_2-25K] showed best result on preliminary examination on conversion rapeseed oil to biodiesel and hence selected for the optimization studies. Furthermore, reaction parameters for the chosen catalyst was optimized to obtain high yield of fatty acid methyl esters (FAME).

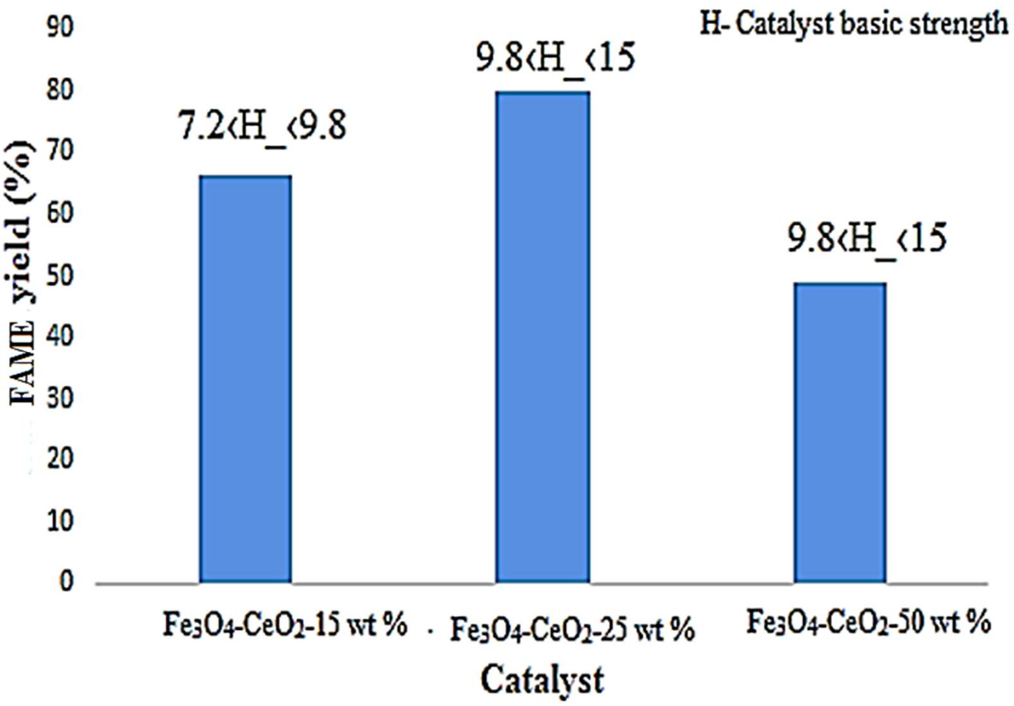

Fig. 1. The efficiency of various catalyst for transesterification of rapeseed oil

3.2. Characterization of catalyst

The FTIR peaks of Fe_3O_4-CeO_2, Fe_3O_4-CeO_2-25K and regenerated Fe_3O_4-CeO_2-25K were shown in Fig.2. The FTIR spectrum observed in region of 3286 cm^{-1} and 1624 cm^{-1} is due to stretching of the –OH group and bending vibration of water molecule respectively[15]. FTIR bands at around 1370 cm^{-1} and 1009 cm^{-1} are due to vibration of CeO_2. The FTIR peaks detected in the range of 500 cm^{-1} to 700 cm cm^{-1} represents Fe–O metal-oxygen bond which indicates the existence of Fe_3O_4 [15]. New peaks at around 833 cm^{-1} and 1390 cm^{-1}indicates impregnation of potassium to the catalyst.

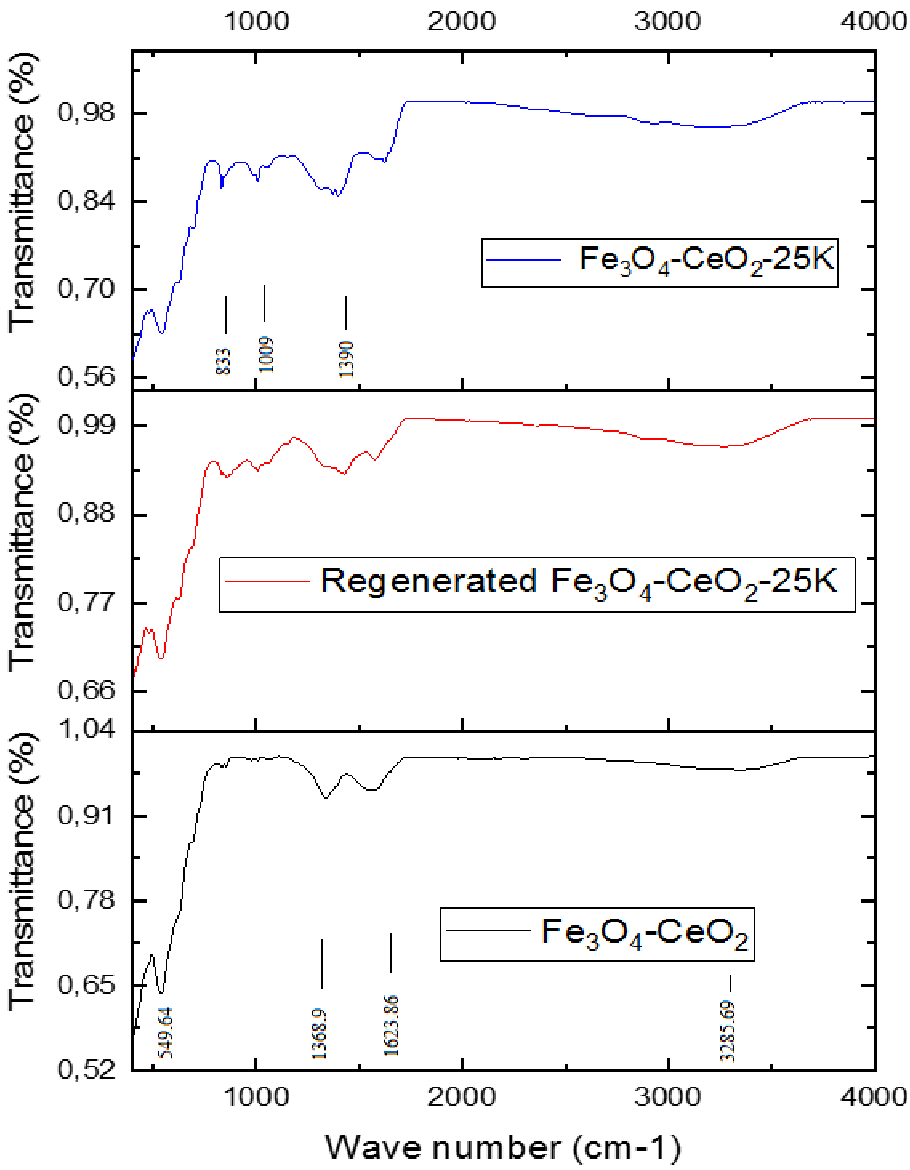

Fig. 2. FTIR spectra of Fe_3O_4-CeO_2, Fe_3O_4-CeO_2-25K and regenerated Fe_3O_4-CeO_2-25K

The Fig. 3 shows the XRD pattern of Fe_3O_4-CeO_2, Fe_3O_4-CeO_2-25K and regenerated Fe_3O_4-CeO_2-25. The regenerated catalyst was obtained by separating catalyst after transesterification. The catalyst was with methanol and heptane to remove impurities and dried at 60 °C and calcined at 500 °C for 4 hours to reactivate the catalyst. X-ray diffraction patterns of Fe_3O_4-CeO_2 depicts peaks at 35.36 °, 41.51 °, 50.8 °, 63.6 °, 67.7 °, 74.7 °. XRD pattern of Fe_3O_4-CeO_2-25K and regenerated Fe_3O_4-CeO_2-25K showed new peaks at 38.72 °, which is due to the impregnation of potassium ions to Fe_3O_4-CeO_2

nanocatalyst [15, 25]. Table 1 shows the crystallographic parameters of Fe_3O_4-CeO_2-25K and regenerated Fe_3O_4-CeO_2-25K after five cycles of transesterification.

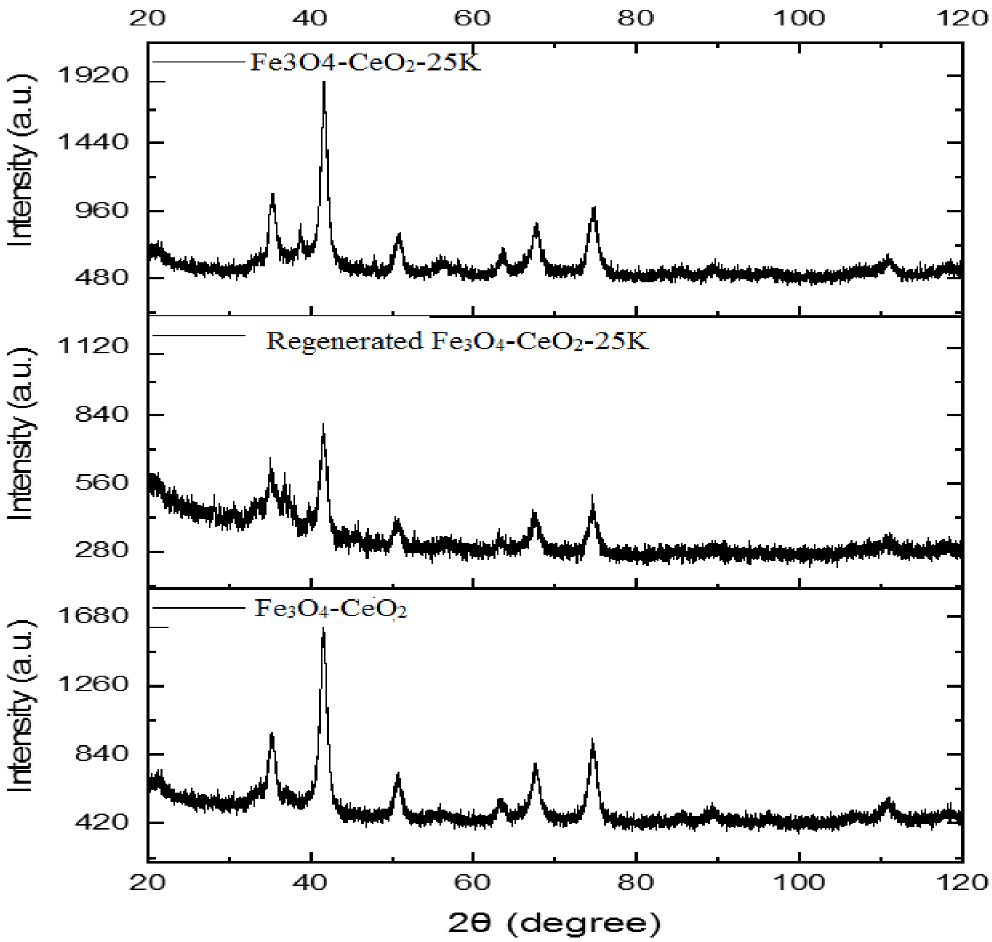

Fig. 3. XRD pattern of Fe_3O_4-CeO_2, Fe3O4-CeO_2-25K and regenerated Fe_3O_4-CeO_2-25K

Table 1.

Catalyst	**Crystal structure**	**a**	**b**	**c**	**α**	**β**	**γ**
		(nm)	(nm)	(nm)			

Fe_3O_4-CeO_2	Hexagonal	0.48	0.48	0.4	90	90	120
Fe_3O_4-CeO_2-25K.	Hexagonal	0.84	0.84	1.2	90	90	120

The crystallographic parameters of Fe_3O_4-CeO_2-25K and regenerated Fe_3O_4-CeO_2-25K

The TEM image of Fe_3O_4-CeO_2 and Fe_3O_4-CeO_2-25K were depicted in Fig. 5a and 5b respectively. The Fe_3O_4-CeO_2 and Fe_3O_4-CeO_2-25K catalyst have a particle size of 20-33.9 nm which was confirmed with help of TEM images. Further after impregnation of potassium ions the flat covered surface was observed. The flat covered surface imply to potassium impregnation. The extension of potassium covering depends on the weight percentage of potassium used for impregnation.

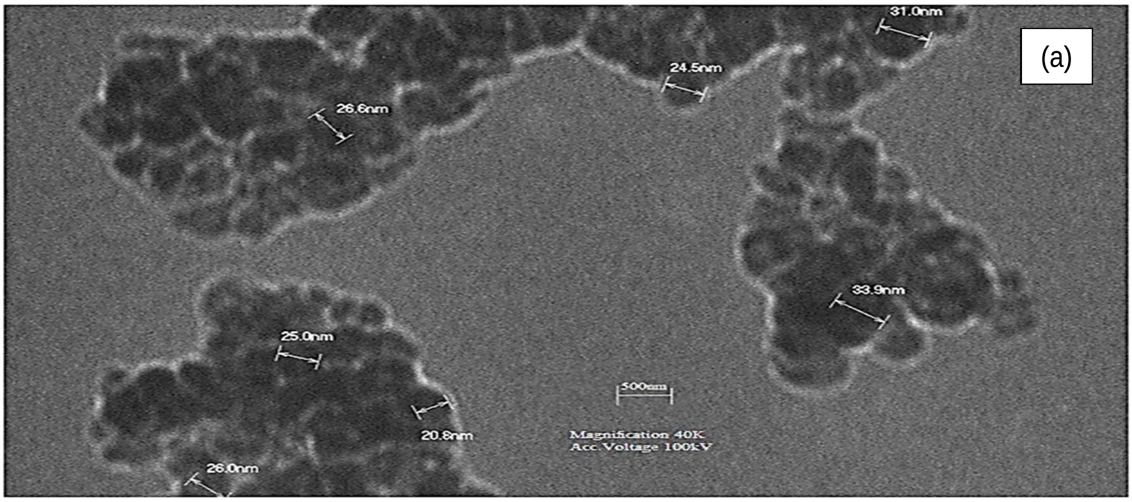

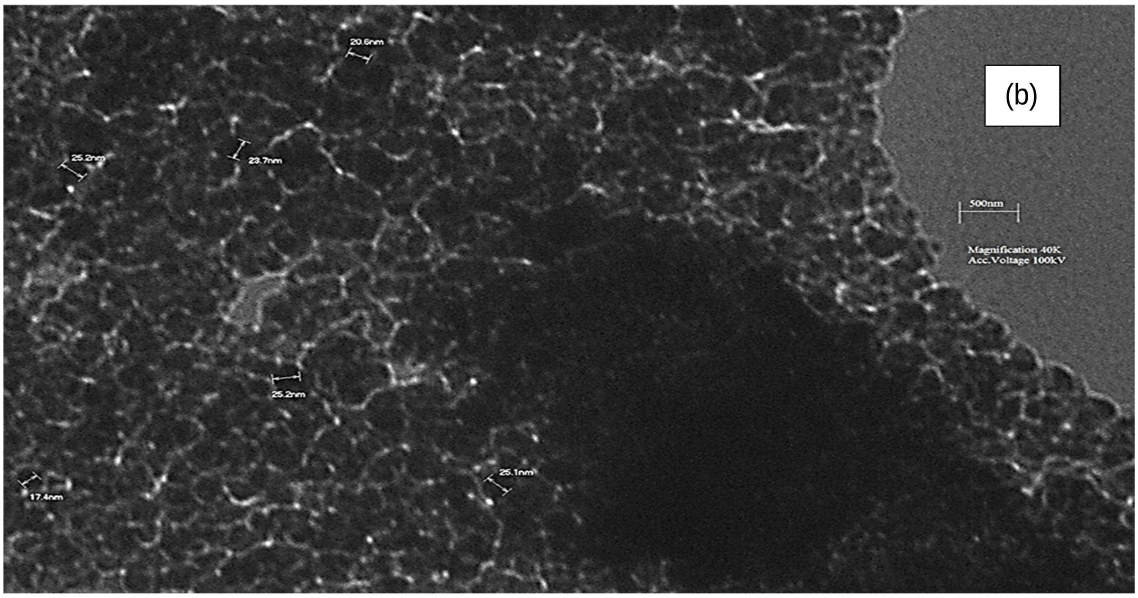

Fig. 4. TEM image of (a) Fe_3O_4-CeO_2 and (b) Fe_3O_4-CeO_2-25K

The composition and surface structure of nanocatalyst were analyzed by SEM. SEM image and EDS graph of Fe_3O_4-CeO_2 and Fe_3O_4-CeO_2-25K provides information about its morphology and elemental composition respectively. By comparing two images, it was observed that there was a coating on the catalyst due to doping of potassium. It also confirms the existence of Fe (34.9 wt %), Ce (13.5 wt %), O (28.8 wt %) and K (16.4 wt %) in the nanocatalyst. The elemental distribution in regenerated catalyst obtained after 5 cycles was found to be Fe (33.5 wt %), Ce (12.9 wt %), O (27.7 wt %) and K (15.4 wt %) in the nanocatalyst.

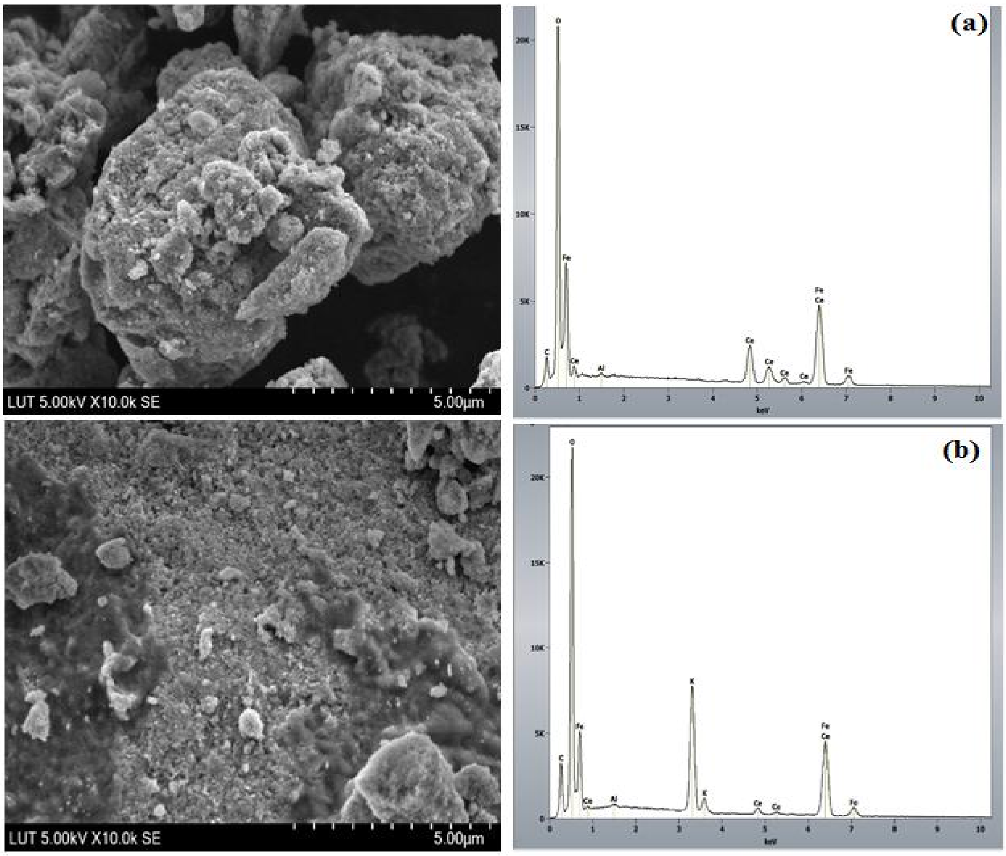

Fig 5. (a) SEM image and EDS of Fe_3O_4-CeO_2 (b) SEM image and EDS of Fe_3O_4-CeO_2-25K

The surface area, pore volume and pore size of Fe_3O_4-CeO_2 and Fe_3O_4-CeO_2-25K were determined by BET analysis. The results of BET analysis of Fe_3O_4-CeO_2 and Fe_3O_4-CeO_2-25K as summarized in Table 2. The BET surface area and pore volume reduced due to loading of potassium and this behavior was quite common with potassium [21, 24, 26].The N_2 adsorption-desorption isotherm for Fe_3O_4-CeO_2 and Fe_3O_4-CeO_2-25K from BET analysis were shown in Fig.6. The hysteretic loop isotherm indicates the presence of mesoporous materials. The pore width and pore volume distribution of Fe_3O_4-CeO_2 and Fe_3O_4-CeO_2-25K depicted in Figure S1.

Table 2 .

The results of Brunauer-Emmett-Teller surface area analysis

	Parameters	Fe_3O_4-CeO_2	Fe_3O_4-CeO_2-25K
Surface area	BET surface area (m^2/g)	80.37	72.84
Pore volume	Single point adsorption total pore volume of pores (cm^3/g)	0.177	0.18
Pore size	Adsorption average pore width (nm)	8.81	9.99

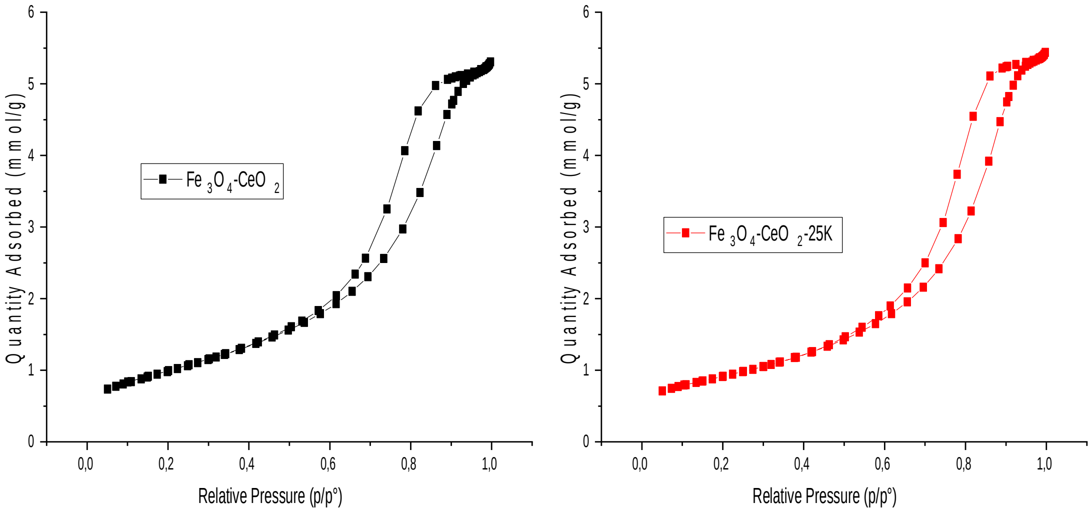

Fig. 6. N_2 adsorption-desorption isotherm plot of Fe_3O_4-CeO_2 and Fe_3O_4-CeO_2-25K

The magnetic properties were measured using SQUID magnetometer (Cryogenic S700X-R, UK). The magnetization versus magnetic field dependencies at 300 Kelvin was obtained for Fe_3O_4-CeO_2-25K shown in Fig.7. The remanent magnetization for Fe_3O_4-

CeO_2-25K sample is 0.75 emu/g. Fig 7 also demonstrates the recovery of catalyst from the reaction mixture.

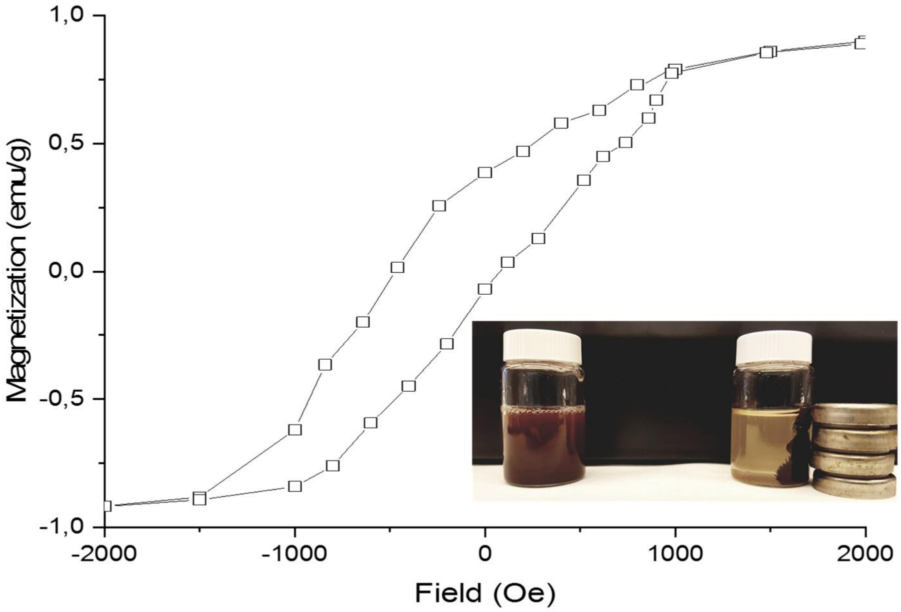

Fig. 7. The magnetization versus magnetic field of Fe_3O_4-CeO_2-25K at 300 K

3.3.Characterization of biodiesel

The quality of synthesized biodiesel should satisfy the criteria determined by ASTM/EN 14214 limits. The fatty acid methyl esters made from the rapeseed oil was characterized by GC-MS, ^{1}H NMR and ^{13}C NMR.

The chemical composition of biodiesel was demonstrated with the help of GCMS chromatogram and National Institute of Standards and Technology (NIST) 2014 MS library. The fatty acid methyl esters obtained after transesterification of rapeseed oil with

Fe_3O_4-CeO_2-25K illustrated in Fig S2. Each FAME peak in the sample was identified with the help of library match and represented in Table S1.

3.3.2 ^{1}H and ^{13}C NMR spectroscopy

^{1}H and ^{13}C NMR spectroscopy was used for the analysis of fatty acid methyl esters derived from rapeseed oil. The conversion was calculated using the equation 2, which was already mentioned above. With the help of ^{1}H NMR, FAME percentage of sample obtained after transesterification of rapeseed oil with Fe_3O_4-CeO_2-25K was found to be 96.13 %. Fig. S3a and S3b demonstrates the ^{1}H NMR and ^{13}C spectrum of fatty acid methyl esters sample obtained with help of Fe_3O_4-CeO_2-25K catalyst respectively. It helps to characterize FAME and can be used to conform the existence of methyl esters in the biodiesel.

In ^{1}H NMR the signal at 3.64 ppm indicates methoxy group (A_{ME}) of FAME and signal at 2.27 ppm corresponding to methylene group (A_{CH2}). The presence of these signal in the biodiesel sample verifies the presence of methyl ester. Apart from the signal used for the quantification, there are other identifiable peaks such as signal at 0.87 to 0.97 ppm for CH_2-CH_3 or for latter methyl group. The peaks in the range of 1.24 to 2.3 represents CH_2 (methylene group). The signals at 5.3 range indicates presence of CH=CH (double bond) groups or olefinic groups[27]. In ^{13}C NMR the signal at the range of 174 ppm and 51 ppm indicates existence of ester carbonyl –COO- and C-O respectively. The unsaturation in biodiesel sample was confirmed with help of signals at 132.11 ppm and 126.89 ppm. The presence of -CH_2 group was showed with help of signals in the region of 21-35 ppm [27].

3.4. Influence of various parameters on biodiesel production

The higher yield of biodiesel was achieved by optimizing the reaction conditions such as oil to methanol ratio, temperature, time, catalyst amount. Based on the preliminary screening of catalysts, the Fe_3O_4-CeO_2-25K catalyst was found to be more capable catalyst for the conversion of rapeseed oil to biodiesel. Series of transesterification reactions were performed using Fe_3O_4-CeO_2-25K in order to achieve the reaction parameters for optimization.

3.4.1 Effect of catalyst amount (weight %) in biodiesel production

The effect of catalyst concentration on biodiesel production was investigated by performing reactions at various catalyst concentration from 1.5 wt % to 6 wt % of oil. The 96.13 % of biodiesel yield was obtained within 120 minutes of reaction time at 65 °C by using 4.5 wt % catalyst and 1:7 oil to methanol molar ratio (Fig. 8a). The conversion of oil to biodiesel raises with increase in amount of catalyst up to 4.5 wt % and extra rise in catalyst concentration beyond the optimum value showed reduction in biodiesel yield due to decrease in the availability of active sites. The additional amount of catalyst aids to saponification of oil which will finally inhibits the reaction[20, 21].

3.4.2 Effect of temperature in biodiesel production

The influence of temperature for high yield reaction which was investigated by conducting reaction at various temperatures using 4.5 wt % catalyst, 1:7 oil to methanol molar ratio for 120 minutes reaction time (Fig. 8b). The yield of biodiesel increased gradually up to 65 °C and resulted in maximum yield of fatty acid methyl esters. After 65 °C biodiesel yield reduced with rise in temperature, which is due to the fact that elevated temperature favors methanol vaporization as well as saponification reaction [20, 28, 29]. Alkaline catalyst favor the saponification of the triglycerides at elevated prior to the completion of the transesterification process [40, 41].

3.4.3 Effect of oil to methanol ratio in biodiesel production

The biodiesel conversion significantly increases as oil to methanol molar ratios were raised from 1:5 to 1:11 illustrated in Fig. 8c. The reaction was carried out at 4.5 wt % catalyst at 65 °C for 120 minutes of reaction time. The biodiesel yield was adversely affected on rising methanol concentration above the optimum amount (1:7) which was due to the higher solubility of glycerol to ester phase resulting in difficulty in separation of biodiesel. The excess amount of methanol than optimum limit leads to increasing the solubility of glycerol into the ester phase thereby encouraging the reverse reaction between glycerol and ester which reduces the yield of biodiesel[30, 31].

3.4.4 Effect of reaction time in biodiesel production

The effect of reaction time on transesterification reaction was observed by executing reactions for various time intervals using 4.5 wt % catalyst, 1:7 oil to methanol molar ratio at 65 °C depicted in Fig. 8d. The fatty acid methyl ester content rose with increase in reaction time up to 120 minutes and reached at its maximum. After 120 minutes FAME percentage remains almost constant, without much reduction in ester content.

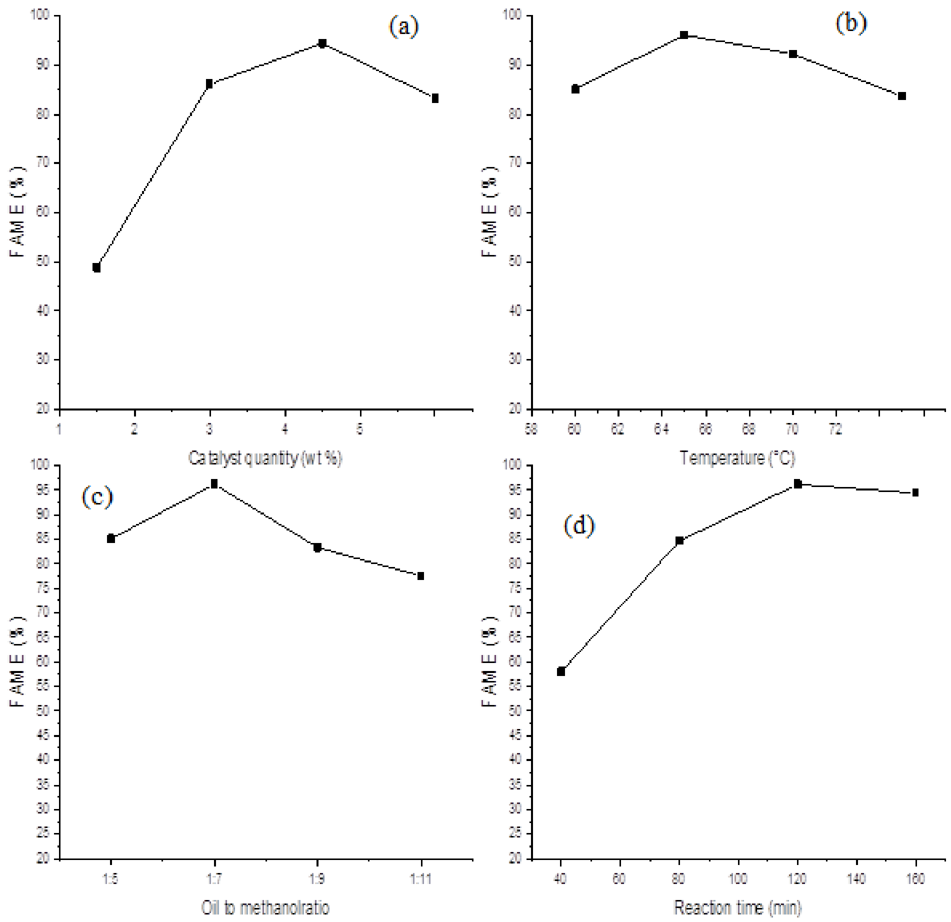

Fig. 8. (a). Effect of catalyst amount (weight %) on FAME yield (b). Effect of reaction temperature on FAME yield (c). Effect of oil to methanol molar ratio on FAME yield (d). Effect of reaction time on FAME yield.

3.5. Properties of synthesized biodiesel from rapeseed oil

The properties of rapeseed oil methyl esters were determined using EN 14214 method as presented in Table 3. All these features play a key role in biodiesel quality. The acid value of rapeseed oil methyl ester was found to be 0.32 mg KOH/g and it was within the limits of European International standard organization (EN ISO) method. The increase in acid value can results in difficulties like corrosion of rubber parts of engine and filter clogging[32]. The density and kinematic viscosity are other two main fuel features which influence the fuel injection operation. Higher values of this factors can negatively affect fuel injection process and leads in the formation of engine deposits[33, 34]. The density and kinematic viscosity of rapeseed oil methyl esters were 880.30 kg/m^3 and 4.37 mm^2/s respectively. The other factor is flash point which specifies the minimum temperature at which fuel starts to ignite. It is vital to know flash point value for fuel handling and storage [35].

Table 3.

Properties of rapeseed oil methyl esters (Fe_3O_4-CeO_2-25K catalyst at concentration of 4.5 wt %, 1:7 oil to methanol ratio, reaction temperature 65 °C, reaction time 120 minutes)

Property	EN 14214 test method	Limits	Methyl ester from rapeseed oil
Acid value (mg KOH/g)	Pr EN14104	0.5 max	0.308
Density at 15°C (kg/m^3)	EN ISO 12185	860-900	880.30
Kinematic viscosity at 40°C mm^2/s	EN ISO 3104	3-5	4.37
Flash point (°C)	EN ISO 2719	-	171°C

3.6. Reusability of catalyst

For an environmental friendly biodiesel production process, the concept of reusability of catalyst is a vital element. The deposition of impurities or oil on catalyst surface and thermal deactivation are typical reasons for catalyst deactivation. The cleaning of catalyst with suitable solvent and calcination helps in its regeneration [36]. To analyze the reusability of Fe_3O_4-CeO_2-25K nanocatalyst, firstly it was separated from rapeseed oil methyl esters and glycerol. After transesterification, the separated catalyst was washed with methanol and heptane to remove impurities. The washed catalyst was dried at 60 °C and calcined at 500 °C for 4hours to reactivate the catalyst. It was detected that activity of catalyst decreased continuously up to the five runs (Fig.9a). It indicates that catalyst activity decreased from 96.13 % to 80.94 % in five cycles. In comparison with earlier reported magnetic nanocatalyst, the synthesized catalyst showed greater yield in biodiesel production [16, 42].

The leaching test was performed to determine the cause of the decrease in activity of synthesized nanocatalyst and its stability. Figure 9b represents the concentration of leached metal ion determined using inductively coupled plasma (ICP, Agilent 5110) after different cycles. The concentration of potassium and cerium in the solution after each cycle were less than 0.56 mg/L and 0.038 mg/L respectively.

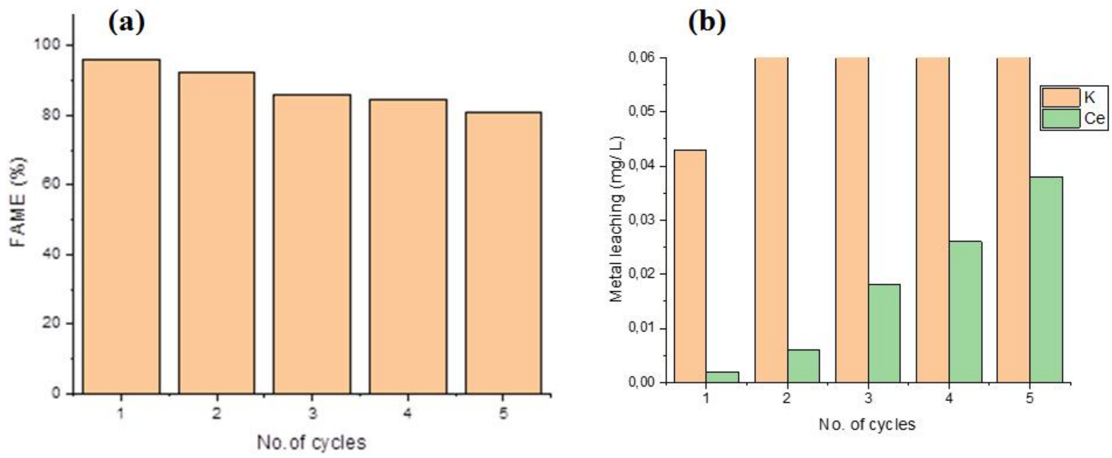

Fig. 9. (a) Reusability analysis and (b) leaching test of Fe_3O_4-CeO_2-25K catalyst up to five transesterification reactions

4. **Conclusion**

The transesterification of rapeseed oil to biodiesel was successfully done with help of Fe_3O_4-CeO_2-25K. The catalytic activity of different weight percentage of potassium impregnated Fe_3O_4-CeO_2 was investigated and best activity was attained at optimum loading of KOH (25wt %) to Fe_3O_4-CeO_2. The characterization of synthesized catalyst and integration of potassium ions to Fe_3O_4-CeO_2 nanostructure confirmed by FTIR, XRD, SEM, TEM. The nanocatalyst showed 96.13 % fatty acid methyl ester content using 4.5

wt % catalyst amount, 1:7 oil to methanol ratio at 65 °C with in a reaction time of 120 minutes. The properties of biodiesel such as acid value, density, kinematic viscosity and flash point were within the EN 14214 limits. All these results, indicates Fe_3O_4-CeO_2-25K is an efficient catalyst for the production of superior quality biodiesel from rapeseed oil as a feedstock. The reusability of catalyst also exhibited favorable result, which makes it cost effective and more eco-friendly. Moreover, the synthesized catalyst was nontoxic and resulted in higher conversion rate of rapeseed oil to biodiesel compared to other magnetic nanocatalyst.

References

[1] A. Demirbas, Biodiesel production from vegetable oils by supercritical methanol, J. Sci. Ind. Res. 64 (2005) 858–865.

[2] J.X. Wang, K.T. Chen, S.T. Huang, K.T. Chen, C.C. Chen, Biodiesel Production from Soybean Oil Catalyzed by Li_2CO_3, (2012) 1619–1625. doi:10.1007/s11746-012-2074-2.

[3] S.P. Singh, D. Singh, Biodiesel production through the use of different sources and characterization of oils and their esters as the substitute of diesel: A review, Renew. Sustain. Energy Rev. 14 (2010) 200–216. doi:10.1016/j.rser.2009.07.017.

[4] E. Bet-Moushoul, K. Farhadi, Y. Mansourpanah, A.M. Nikbakht, R. Molaei, M. Forough, Application of CaO-based/Au nanoparticles as heterogeneous nanocatalysts in biodiesel production, Fuel. 164 (2016) 119–127. doi:10.1016/j.fuel.2015.09.067.

[5] G. Huang, F. Chen, D. Wei, X. Zhang, G. Chen, Biodiesel production by microalgal biotechnology, Appl. Energy. 87 (2010) 38–46. doi:10.1016/j.apenergy.2009.06.016.

[6] M.E. Hums, R.A. Cairncross, S. Spatari, Life-Cycle Assessment of Biodiesel Produced from Grease Trap Waste, Environ. Sci. Technol. 50 (2016) 2718–2726. doi:10.1021/acs.est.5b02667.

[7] A. Abbaszaadeh, B. Ghobadian, M.R. Omidkhah, G. Najafi, Current biodiesel production technologies : A comparative review, Energy Convers. Manag. 63 (2012) 138–148. doi:10.1016/j.enconman.2012.02.027.

[8] G. Baskar, R. Aiswarya, Trends in catalytic production of biodiesel from various feedstocks, Renew. Sustain. Energy Rev. 57 (2016) 496–504. doi:10.1016/j.rser.2015.12.101.

[9] L. Wen, Y. Wang, D. Lu, S. Hu, H. Han, Preparation of KF / CaO nanocatalyst and its application in biodiesel production from Chinese tallow seed oil, Fuel. 89 (2010) 2267–2271. doi:10.1016/j.fuel.2010.01.028.

[10] R. Madhuvilakku, S. Piraman, Biodiesel synthesis by TiO_2-ZnO mixed oxide nanocatalyst catalyzed palm oil transesterification process, Bioresour. Technol. 150 (2013) 55–59. doi:10.1016/j.biortech.2013.09.087.

[11] S. Ben, F. Zhao, Z. Safaei, I. Babu, D. Lakshmi, M. Sillanpää, Applied Catalysis B : Environmental Reactivity of novel Ceria – Perovskite composites CeO_2 - $LaMO_3$ (MCu , Fe) in the catalytic wet peroxidative oxidation of the new emergent pollutant “ Bisphenol F ”: Characterization , kinetic and mechanism studies, "Applied Catal. B, Environ. 218 (2017) 119–136. doi:10.1016/j.apcatb.2017.06.047.

[12] B. Gao, Z. Safaei, I. Babu, S. Iftekhar, E. Iakovleva, V. Srivastava, B. Doshi, S. Ben, S. Kalliola, Journal of Photochemistry and Photobiology A : Chemistry Modi fi cation of $ZnIn_2S_4$ by anthraquinone-2-sulfonate doped polypyrrole as acceptor-donor system for enhanced photocatalytic degradation of tetracycline, "Journal Photochem. Photobiol. A Chem. 348 (2017) 150–160. doi:10.1016/j.jphotochem.2017.08.037.

[13] I. Ambat, V. Srivastava, M. Sillanpää, Recent advancement in biodiesel production methodologies using various feedstock : A review, 90 (2018) 356–369.

[14] A. Lu, E.L. Salabas, F. Schüth, Magnetic Nanoparticles : Synthesis , Protection , Functionalization , and Application Angewandte, (2007) 1222–1244. doi:10.1002/anie.200602866.

[15] A. Gogoi, M. Navgire, K. Chandra, P. Gogoi, Fe_3O_4-CeO_2 metal oxide nanocomposite as a Fenton-like heterogeneous catalyst for degradation of catechol, Chem. Eng. J. 311 (2017) 153–162. doi:10.1016/j.cej.2016.11.086.

[16] S. Hu, Y. Guan, Y. Wang, H. Han, Nano-magnetic catalyst KF/CaO-Fe_3O_4 for biodiesel production, Appl. Energy. 88 (2011) 2685–2690. doi:10.1016/j.apenergy.2011.02.012.

[17] V. Srivastava, T. Kohout, M. Sillanpää, Journal of Environmental Chemical Engineering Potential of cobalt ferrite nanoparticles ($CoFe_2O_4$) for remediation of hexavalent chromium from synthetic and printing press wastewater, Biochem. Pharmacol. 4 (2016) 2922–2932. doi:10.1016/j.jece.2016.06.002.

[18] L.H.A. and H.E.T. M.F.C. Andrade, A.L.A. Parussulo, C.G.C.M. Netto, Lipase immobilized on polydopamine-coated magnetite nanoparticles for biodiesel production from soybean oil, Biofuel Res. J. 10 (2016) 403–409. doi:10.18331/BRJ2016.3.2.5.

[19] M. Akia, F. Yazdani, E. Motaee, D. Han, H. Arandiyan, A review on conversion of biomass to biofuel by nanocatalysts, Nanocatalysts. Biofuel Res. J. Biofuel Res. J. 1 (2014) 16–25.

[20] V. Singh, F. Bux, Y.C. Sharma, A low cost one pot synthesis of biodiesel from waste frying oil (WFO) using a novel material, β-potassium dizirconate (β-$K_2Zr_2O_5$), Appl. Energy. (2016). doi:10.1016/j.apenergy.2016.02.135.

[21] M. Takase, Y. Chen, H. Liu, T. Zhao, L. Yang, X. Wu, Biodiesel production from non-edible Silybum marianum oil using heterogeneous solid base catalyst under ultrasonication, Ultrason. Sonochem. 21 (2014) 1752–1762. doi:10.1016/j.ultsonch.2014.04.003.

[22] N. Pereira, F. Sávio, G. Pereira, C.C. Galvão, A. Maria, R. Bastos, V. Lins, M. Aparecida, N. Medeiros, D.L. Filho, Biodiesel from Residual Oils : Less Environmental Impact with Sustainability and Simplicity, 17 (2016) 1–14. doi:10.9734/CSIJ/2016/29455.

[23] F. Qiu, Y. Li, D. Yang, X. Li, P. Sun, Heterogeneous solid base nanocatalyst: Preparation, characterization and application in biodiesel production, Bioresour. Technol. 102 (2011) 4150–4156. doi:10.1016/j.biortech.2010.12.071.

[24] Y. Li, F. Qiu, D. Yang, X. Li, P. Sun, Preparation, characterization and application of heterogeneous solid base catalyst for biodiesel production from soybean oil, Biomass and Bioenergy. 35 (2011) 2787–2795. doi:10.1016/j.biombioe.2011.03.009.

[25] D. Salinas, G. Pecchi, V. Rodríguez, J. Luis, G. Fierro, Effect of Potassium on Sol-Gel Cerium and Lanthanum Oxide Catalysis for Soot Combustion, (2015) 68–77.

[26] F. Qiu, Y. Li, D. Yang, X. Li, P. Sun, Bioresource Technology Heterogeneous solid base nanocatalyst : Preparation , characterization and application in biodiesel production, 102 (2011) 4150–4156. doi:10.1016/j.biortech.2010.12.071.

[27] M. Tariq, S. Ali, N. Khalid, Activity of homogeneous and heterogeneous catalysts, spectroscopic and chromatographic characterization of biodiesel: A review, Renew. Sustain. Energy Rev. 16 (2012) 6303–6316. doi:10.1016/j.rser.2012.07.005.

[28] E.C. Abbah, G.I. Nwandikom, C.C. Egwuonwu, N.R. Nwakuba, Effect of Reaction Temperature on the Yield of Biodiesel From Neem Seed Oil, Am. J. Energy Sci. 3 (2016) 16–20.

[29] T. Eevera, K. Rajendran, S. Saradha, Biodiesel production process optimization and characterization to assess the suitability of the product for varied environmental conditions, Renew. Energy. 34 (2009) 762–765. doi:10.1016/j.renene.2008.04.006.

[30] G. Kafui, A. Sunnu, J. Parbey, Effect of biodiesel production parameters on viscosity and yield of methyl esters : Jatropha curcas , Elaeis guineensis and Cocos nucifera, Alexandria Eng. J. 54 (2015) 1285–1290. doi:10.1016/j.aej.2015.09.011.

[31] F.F. Banihani, Transesterification and Production of Biodiesel from Waste

Cooking Oil : Effect of Operation Variables on Fuel Properties, 4 (2017) 154–160. doi:10.11648/j.ajche.20160406.13.

[32] A.B. Chhetri, M.S. Tango, S.M. Budge, K.C. Watts, M.R. Islam, Non-edible plant oils as new sources for biodiesel production, Int. J. Mol. Sci. 9 (2008) 169–180. doi:10.3390/ijms9020169.

[33] G. Knothe, K.R. Steidley, Kinematic viscosity of biodiesel fuel components and related compounds. Influence of compound structure and comparison to petrodiesel fuel components, Fuel. 84 (2005) 1059–1065. doi:10.1016/j.fuel.2005.01.016.

[34] A. Demirbas, Biodiesel: A realistic fuel alternative for diesel engines, Biodiesel A Realis. Fuel Altern. Diesel Engines. (2008) 1–208. doi:10.1007/978-1-84628-995-8.

[35] H.G. Aleme, P.J.S. Barbeira, Determination of flash point and cetane index in diesel using distillation curves and multivariate calibration, Fuel. 102 (2012) 129–134. doi:10.1016/j.fuel.2012.06.015.

[36] W. V. Prescott, A.I. Schwartz, Nanorods and Nanomaterials Research Progress, (2008) 279. http://books.google.es/books/about/Nanorods_Nanotubes_and_Nanomaterials_Res.html?id=a2De3CXrM8wC&pgis=1.

[37] Zhang N, Xue H, Hu R., The activity and stability of CeO_2 @ CaO catalysts for the production of biodiesel, RSC Advances. 8 (2018) 32922–32929. doi:10.1039/c8ra06884d.

[38] Mangkin M, Berpenyokong D., Optimization of process parameters for the production of biodiesel from waste cooking oil in presence of bifunctional γ-Al_2O_3-CeO_2 supported catalysts ,The Malaysian Journal of Analytical Sciences, 19(2015) , 8–19.

[39] Orozco LM, Renz M, Corma A., Cerium oxide as a catalyst for the ketonization of aldehydes: mechanistic insights and a convenient way to alkanes without the consumption of external hydrogen, 19 (2017):1555–1569.

doi:10.1039/c6gc03511f.

[40] Eloka-eboka AC, Igbum OG, Inambao FL., Optimization and effects of process variables on the production and properties of methyl ester biodiesel, Journal of Energy in Southern Africa , 25 (2014), 39–47.

[41] Saha R, Goud V V., Ultrasound assisted transesterification of high free fatty acids karanja oil using heterogeneous base catalysts, Biomass Conv. Bioref., 5 (2015), 195-207. doi:10.1007/s13399-014-0133-7.

[42] Feyzi M, Nourozi L, Zakarianezhad M. Preparation and characterization of magnetic $CsH_2PW_{12}O40/Fe–SiO_2$ nanocatalysts for biodiesel production., Materials Research Bulletin 60 (2014) 412–420, doi:10.1016/j.materresbull.2014.09.005.

Nano-magnetic potassium impregnated ceria as catalyst for the biodiesel production.

Indu Ambat [a]*, Varsha Srivastava [a], Esa Haapaniemi [c], Mika Sillanpää [a, b]

[a] Department of Green Chemistry, School of Engineering Science, Lappeenranta University of Technology, Sammonkatu 12, FI-50130 Mikkeli, Finland

[b] Department of Civil and Environmental Engineering, Florida International University, Miami, FL-33174, USA

[c] Department of Organic Chemistry, University of Jyväskylä, Finland

*Corresponding Author (email: indu.ambat@lut.fi)

Supplementary materials

Tables

Table S1.

The composition of biodiesel obtained after transesterification with Fe_3O_4-CeO_2-25K

Peak	Retention time(minutes)	Library match (%)	Mass spectrum with compound
1	8.35	91.77	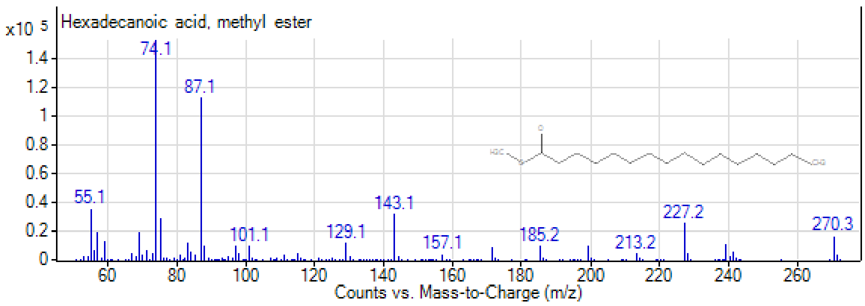

2	9.87	92.74	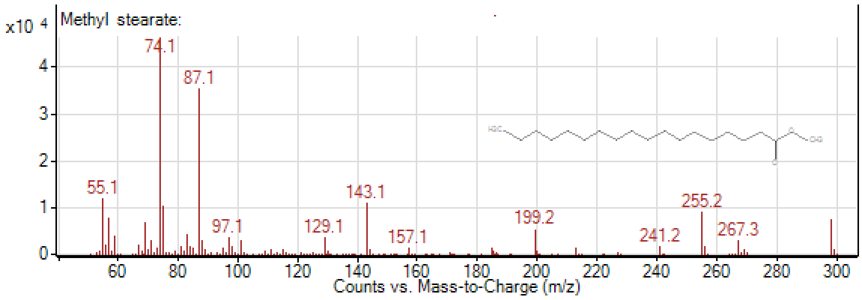
3	10.09	93.73	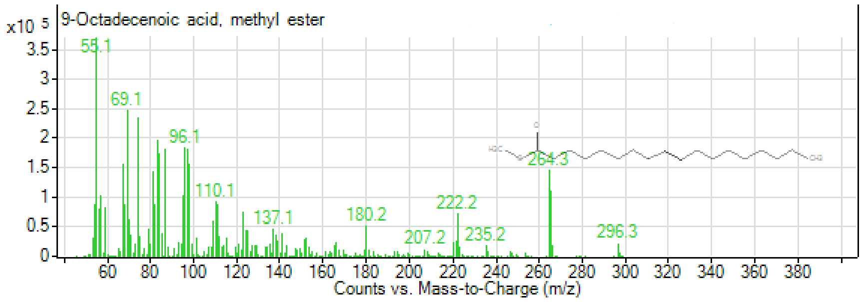
4	10.51	96.67	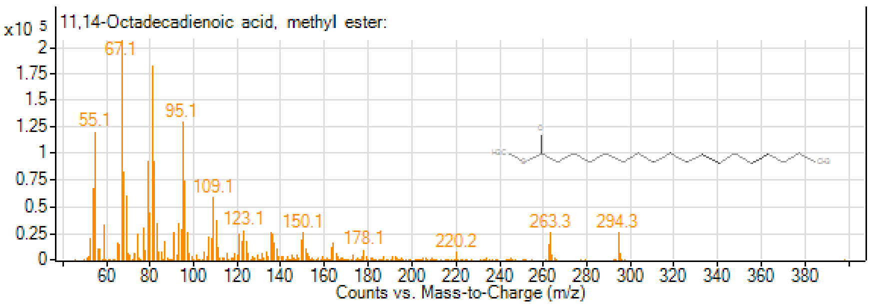
5	11.19	92.22	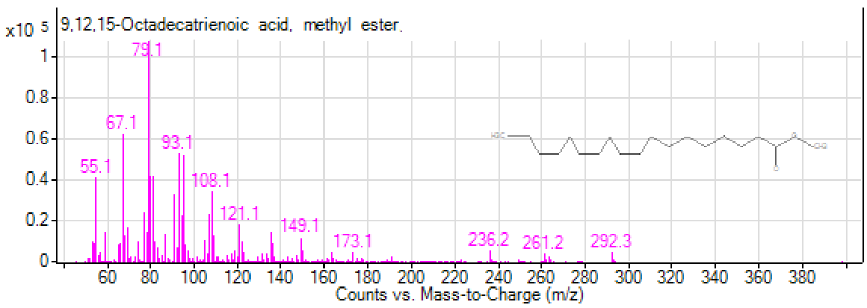
6	12.02	88.15	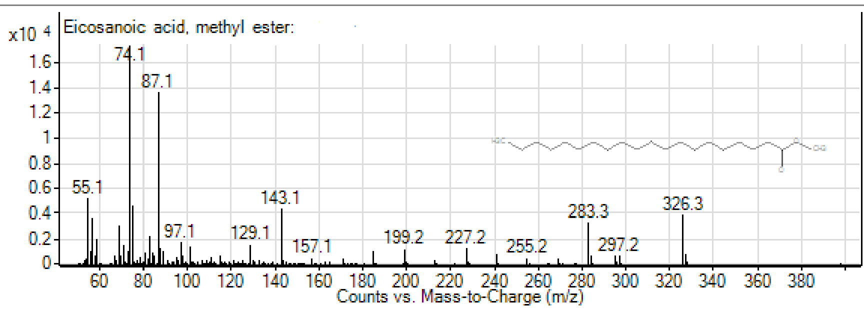

7	12.25	92.08	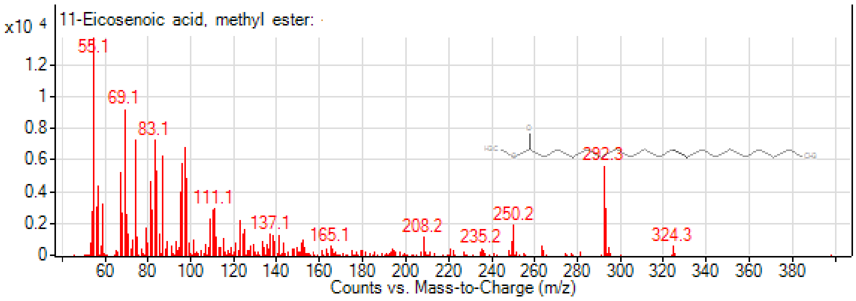 x10 4 11-Eicosenoic acid, methyl ester: 55.1 69.1 83.1 111.1 137.1 165.1 208.2 235.2 250.2 292.3 324.3 Counts vs. Mass-to-Charge (m/z)

Nano-magnetic potassium impregnated ceria as catalyst for the biodiesel production.

Indu Ambat [a]*, Varsha Srivastava [a], Esa Haapaniemi [c], Mika Sillanpää [a, b]

[a] Department of Green Chemistry, School of Engineering Science, Lappeenranta University of Technology, Sammonkatu 12, FI-50130 Mikkeli, Finland

[b] Department of Civil and Environmental Engineering, Florida International University, Miami, FL-33174, USA

[c] Department of Organic Chemistry, University of Jyväskylä, Finland

*Corresponding Author (email: indu.ambat@lut.fi)

Supplementary materials

Figures

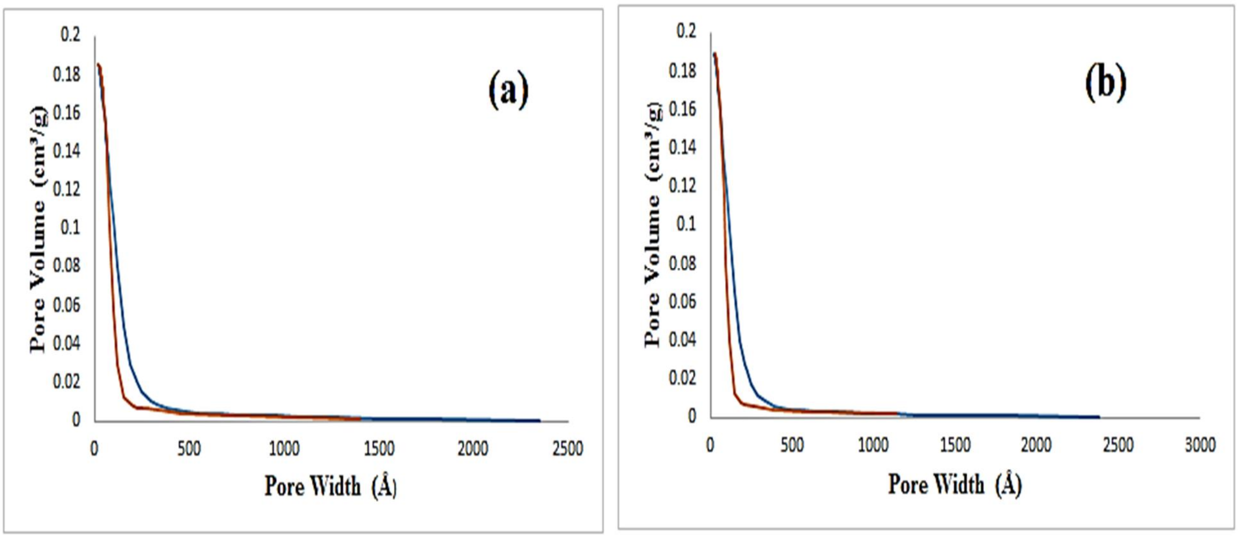

Fig. S1. Pore volume and pore width distribution of Fe_3O_4-CeO_2 and Fe_3O_4-CeO_2-25K

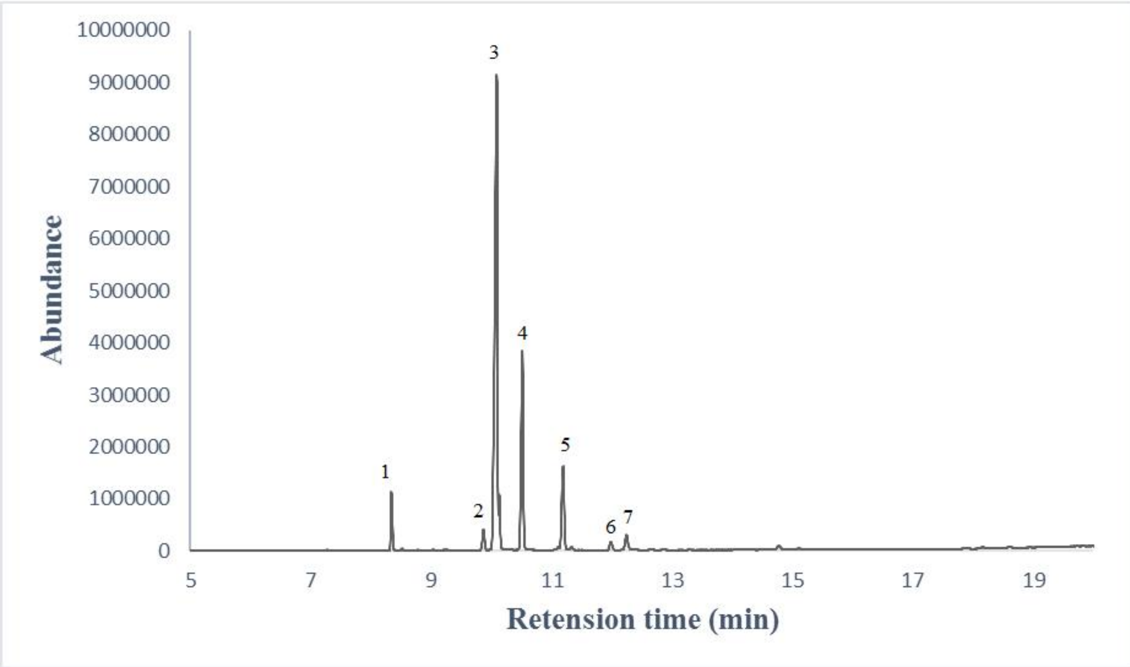

Fig. S2. Illustrates GC-MS spectrum of biodiesel obtained after transesterification with 4.5 wt % Fe_3O_4-CeO_2-25K, 1:7 oil to methanol molar ratio at 65 °C for 120 minutes.

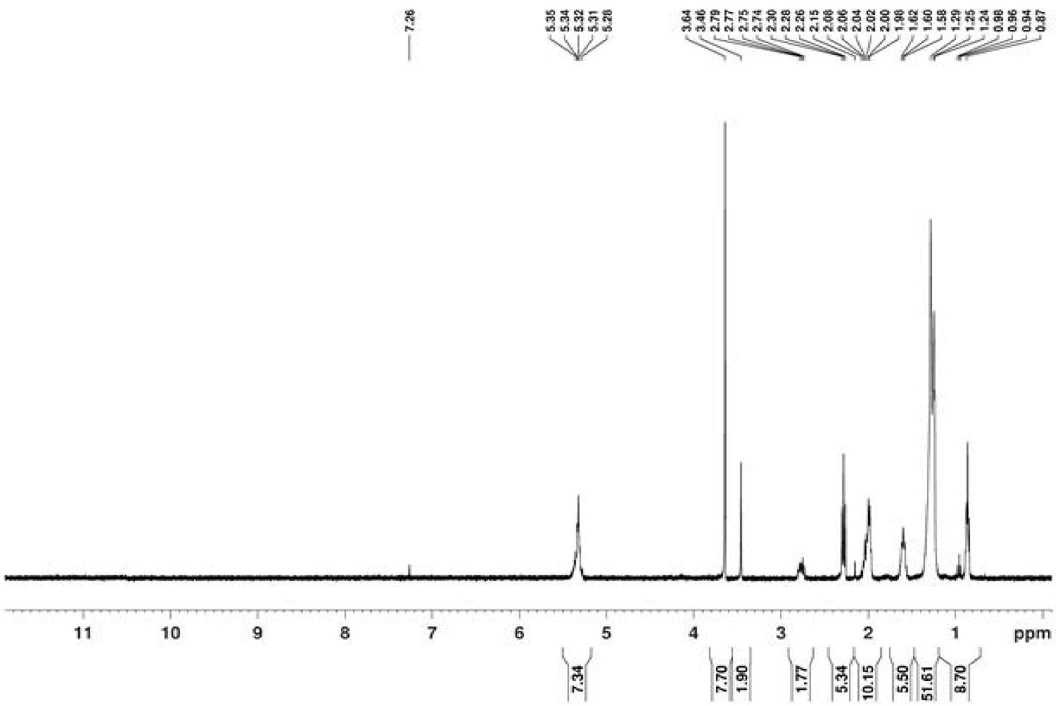

Fig. S3 a. The ^{1}H NMR for the biodiesel sample obtained with Fe_3O_4-CeO_2-25K

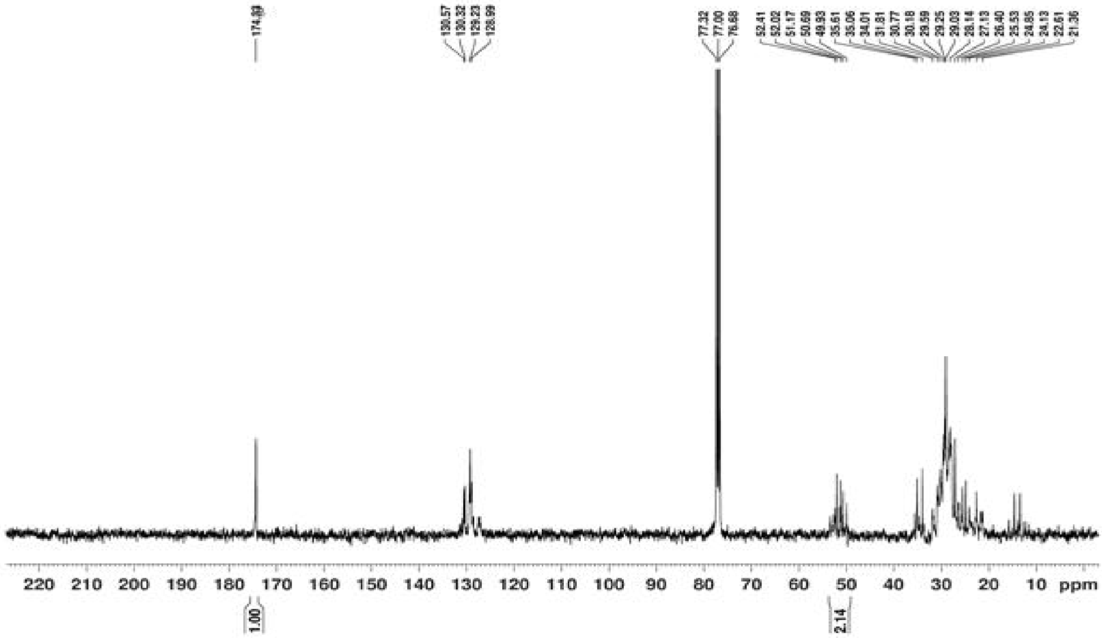

Fig. S3 b. The ^{13}C NMR for the biodiesel sample obtained with Fe_3O_4-CeO_2-25K